

A fragmentation study of kaempferol using electrospray quadrupole time-of-flight mass spectrometry at high mass resolution

Raymond E. March*, Xiu-Sheng Miao

Department of Chemistry, Water Quality Centre, Trent University, 1600 West Bank Drive, Peterborough, Ont., Canada K9J 7B8

Received 13 May 2003; accepted 11 October 2003

Dedicated to Professor Jean-Claude Tabet on the occasion of his 60th birthday

Abstract

A mass spectrometric method based on the combined use of electrospray ionization, collision-induced dissociation and tandem mass spectrometry at high mass resolution has been applied to an investigation of the structural characterization of protonated and deprotonated kaempferol (3,5,7,4'-tetrahydroxyflavone). Low-energy product ion mass spectra of $[M + H]^+$ ions showed simple fragmentations of the C ring that permitted characterization of the substituents in the A and B rings. In addition, four rearrangement reactions accompanied by losses of C_2H_2O , CHO^\bullet , CO , and H_2O were observed. Low-energy product ion mass spectra of $[M - H]^-$ ions showed only four rearrangement reactions accompanied by losses of OH^\bullet , CO , CH_2O , and C_2H_2O . The use of elevated cone voltages permitted observation of product ion mass spectra of selected primary and secondary fragment ions so that each fragment ion reported was observed as a direct product of its immediate precursor ion. Product ion mass spectra examined at high mass resolution allowed unambiguous determination of the elemental composition of fragment ions and resolution of two pairs of isobars. Fragmentation mechanisms and ion structures have been proposed.

© 2004 Elsevier B.V. All rights reserved.

Keywords: Kaempferol; Tandem mass spectrometry; Flavonoid; Accurate mass; Electrospray ionization

1. Introduction

The study of the ubiquitous class of phytochemicals known as the flavonoids has been confined largely heretofore to their distribution in the plant kingdom, elucidation of their structures, and the pathways by which they are synthesized. Flavonoid is a collective noun given to several classes of structurally similar, naturally-occurring compounds; the major classes are flavones, isoflavones, flavans, anthocyanins, proanthocyanidins, flavanones, chalcones, and aurones. The flavonoids were reviewed extensively in 1994 [1]. Plants synthesize flavonoids, along with other secondary metabolites for protection against pathogens and herbivores. Flavonoids are ubiquitous in the environment; they are found primarily in petals, the foliage of trees and bushes, and are widely distributed in the edible parts of plants.

Flavonoids may be of ecotoxicological importance since they are present in the heartwood of tree species used for wood pulp [2,3] and are to be found in a variety of fruits, vegetables and Graminae (e.g., soy) that are important components of the diets of humans and animals [4,5]. Flavonoids are of environmental significance because several flavonoid aglycones (flavonoid glycosides that have lost the sugar moiety) are known to be biologically active [6] while some isoflavones are also phytoestrogens, that is, they mimic the sex hormone estrogen. While phytochemicals in the heartwood and sapwood of trees make the wood disease-resistant [2], flavonoids can affect reproduction in mammals by acting upon the pituitary–gonadal axis, either as competitors for steroid receptor sites [7] or by inhibiting aromatase [8]. Flavonoids are present also in herbal medicines [9] and preventative therapeutics [10]. The existence of these compounds as monomers, dimers and trimers has been linked to increased antioxidant activity [11]. The potential health effects of flavonoids demand that methods be developed for their determination and quantification in food products, plant extracts, and serum.

* Corresponding author. Tel.: +1-705-748-1011/5886;
fax: +1-705-748-1625.

E-mail address: rmarch@trentu.ca (R.E. March).

The advent of fast atom bombardment (FAB), atmospheric pressure chemical ionization (APCI), and electrospray ionization (ESI) combined with tandem mass spectrometry (MS/MS) has permitted ready study of the flavonoids, their ion chemistry, and the determination of flavonoids in low concentrations in aqueous systems. Mass spectrometric methods coupled to liquid chromatography show great promise for the analysis and quantification of these compounds in biological samples [12–15], food products [16], plant extracts [17–19], and for fundamental studies [20–26]. Thermospray LC/MS/MS has been used for the characterization of flavonoids [27] and the rapid screening of fermentation broths for flavones [28]. Using ion spray LC/MS/MS, parent ion scans of the two protonated aglycones, quercetin and kaempferol, indicated the presence of more than 12 different flavonol glycosides among nine hop varieties [29]. Ion spray LC/MS/MS has been used also for the characterization of flavonoids in extracts from *Passiflora incarnata* [30,31]. APCI/MS/MS has been employed for the quantitative analysis of xanthohumol and related prenylflavonoids in hops and beer [32], for a study of flavonone absorption following naringin, hesperidin, and citrus administration [33] and for the identification of 26 aglycones from the leaf surfaces of *Chrysothamnus* [34]. ES/MS/MS has been employed for the investigation of 14 flavonoids [35], apigenin anionic clusters in the gas phase [36] and of Na⁺-bound clusters of quercetin in the gas phase [37]. The combination of MS/MS with these ionization techniques for polar compounds has proven to be a valuable technique that has great sensitivity, specificity, mass range, and mass resolution.

Kaempferol was selected for this study because it is a multiply-substituted flavonoid aglycone and exemplifies the behavior of aglycones. The examination of kaempferol is a necessary base-line study for our current examination of flavonoid glycosides. This fragmentation study of kaempferol (3,5,7,4'-tetrahydroxyflavone) consists of an examination of the fragmentation of protonated kaempferol and deprotonated kaempferol formed by ESI. The mass/charge ratios of the fragment ions were obtained at high mass resolution to within 0.1 mDa. Pathways for the formation of primary fragment ions are proposed. The signal ion intensities of primary fragment ions were maximized by variation of the cone voltage. Each of the primary ion species obtained thus was isolated in the mass-resolving quadrupole mass filter and fragmented further in the collision cell. This process of examination of primary, secondary, and tertiary ions was continued until prevented by lack of ion signal intensity. While precise mass/charge ratios of fragment ions of low mass/charge ratio were difficult to obtain due to low signal ion intensity, each fragment ion reported was observed as a direct product of its immediate precursor ion. Ion structures have been proposed for each of the fragments observed in each fragmentation series. The same mass spectrometric procedure was applied to an examination of [M – H][–] ions of kaempferol.

2. Experimental

2.1. Materials

Kaempferol was purchased from Sigma (St. Louis, MO, USA). Methanol was purchased from Fisher (Fair Lawn, NJ, USA). The analyte solution was prepared using methanol and water (1:1) at a concentration of 100 µg ml^{–1}. Kaempferol has relatively low stability and it is recommended that the solid material be kept in a freezer. The solutions of kaempferol in methanol and water (1:1) are also unstable. Despite keeping the solutions refrigerated overnight, it was necessary to prepare fresh solutions each day in order to obtain reproducible results. The solution was infused to the ESI source using a Harvard Apparatus Model 11 syringe pump (Harvard Apparatus, Holliston, MA) at a flow rate of 10 µl min^{–1}.

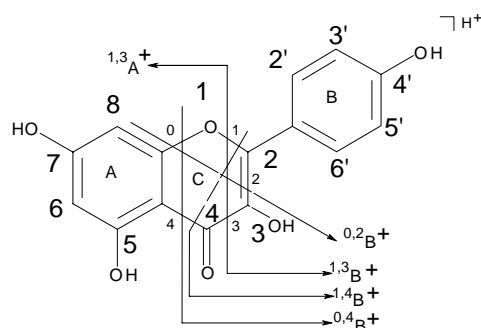
2.2. ESI mass spectrometry

ESI/MS and MS/MS experiments were performed on a Q-TOF 2TM mass spectrometer with a Z-sprayTM ESI source (Micromass, Manchester, UK). The ESI source potentials were: capillary 3.0 kV and extractor 2 V. The sampling cone voltage was varied from 20 to 140 V for ESI mass spectra and the specific value for each collision-induced dissociation (CID) experiment is given in the text. The quadrupole mass filter to the TOF analyzer was set with LM and HM resolution of 15.0 (arbitrary units), which is equivalent to a 1.0 Da mass window for transmission of precursor ions. The source block and desolvation temperatures were set at 80 and 150 °C, respectively. All single analyzer mass spectra were obtained by scanning the TOF analyzer. CID of mass-selected ions were performed in an rf-only quadrupole collision cell. UHP argon was used as the collision gas at 10 psi inlet pressure for CID experiments. Signal detection was performed with a reflector, microchannel plate (MCP) detector and time-to-digital converter. Mass calibration was carried out using a NaI/CsI standard solution from *m/z* 50–1000. Data acquisition and processing were carried out using software MassLynx NT version 3.5 supplied with the instrument. The MS survey range was *m/z* 50–1000, with a scan duration of 1.0 s and an interscan delay of 0.1 s. Each mass spectrum was recorded over a period of 1 s and mass spectra were accumulated over a period of at least 60 s for both single analyzer profiles and CID experiments. For each of the ion species examined, the lock mass in each product ion mass spectrum was the calculated monoisotopic mass/charge ratio of the precursor ion.

3. Results and discussion

3.1. Nomenclature

The nomenclature system for flavonoid aglycones, as developed by Mabry and Markham [38] for the definition of



Scheme 1. Structure of protonated kaempferol, nomenclature and principal fragmentations.

the various A and B ring fragments generated by EI, was found to be inadequate for describing the range of product ions formed when protonated molecules are subjected to CID [39,40]. A more systematic ion nomenclature for flavonoid aglycones has been proposed [41] that is conceptually similar to that introduced for the description of carbohydrate fragmentations in product ion mass spectra of glycoconjugates [42]. For free aglycones, the $^{i,j}A^+$ and the $^{i,j}B^+$ labels designate primary product ions containing intact A and B rings, respectively, in which the superscripts indicate the C-ring bonds that have been broken. In Scheme 1, the C-ring bonds are numbered with a small font, the carbon atoms in all three rings are labeled with a larger font, and the primary fragmentations are indicated.

3.2. Protonated kaempferol

The product ion mass spectrum for protonated kaempferol, m/z 287, obtained at a collision energy of 30 eV is shown in Fig. 1. Initially, the collision energy was maintained at 4 eV so as to transmit protonated kaempferol ions in order to obtain a well-shaped peak for this ion species; then,

after 1 min, the collision energy was increased to 30 eV for the following 3 min in order to observe the fragment ions of m/z 287. The parent ion peak (m/z 287.0556) was used as a lock mass for the product ion mass spectrum of Fig. 1. The structure of kaempferol is given in Scheme 1. The product ion mass spectrum for protonated kaempferol (Fig. 1) obtained with an ES source is essentially similar to the low-energy CID spectrum reported by Claeys and co-workers [41] and obtained by fast atom bombardment (FAB) using cesium ions with an impact energy of ≈ 22 keV, except for one major fragment ion. The ion species of m/z 258, formed by loss of CHO^\bullet from m/z 287, was observed only in the ES product ion mass spectrum.

The primary product ions of the fragmentation of protonated kaempferol are shown in Scheme 2. Nine primary product ions were observed and it is proposed that these ion species are formed in seven fragmentation pathways. These pathways are examined below. In Table 1 are tabulated the formula, observed mass, calculated mass, double bond equivalents, and mass error for the fragment ions observed in the product ion mass spectra of protonated kaempferol. The errors between the observed and calculated masses ranged from 0 to 8.0 mDa (0–33.0 ppm) with an average value of 1.9 mDa (9.9 ppm) indicating good mass accuracy. It should be noted that a mass defect of 1.0 mDa for an ion of low mass/charge ratio, say m/z 200, yields an error of 5 ppm which is not inordinately high for small mass/charge ratio ions. Furthermore, for an ion of m/z 200, there are few different elemental compositions that satisfy the requirements of the elemental composition of the known parent ion therefore the elemental composition of a fragment ion can be obtained with a high degree of confidence.

It is believed that the presentations of the structures proposed by Claeys and co-workers for the $^{0,2}A^+$, $^{0,2}A^+ - CO$, and $^{0,2}B^+$ ions in Scheme 7 of [41] are in error; in order to comply with the given mass/charge ratios and the

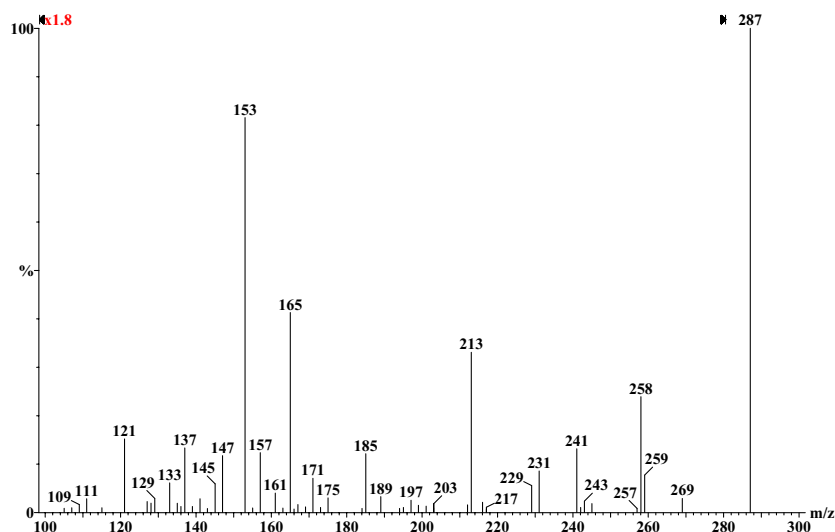
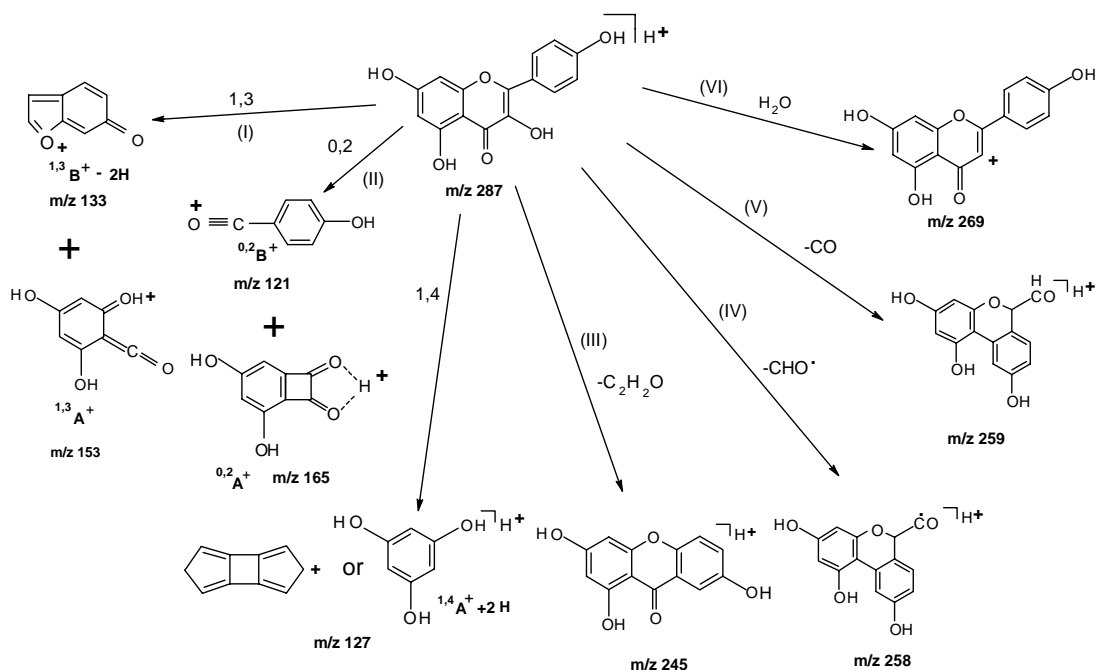


Fig. 1. Product ion mass spectrum of protonated kaempferol obtained at a laboratory frame collision energy of 30 eV.



Scheme 2. Primary fragmentations of protonated kaempferol.

nomenclature of the ions, the $^{0,2}A^+$ and $^{0,2}A^+ - CO$ ion structures should each show one additional degree of unsaturation and the $^{0,2}B^+$ ion structure should show one less oxygen atom. The structures for the $^{0,2}A^+$ and $^{0,2}B^+$ ions given in Scheme 2 and for the $^{0,2}A^+ - CO$ ion given in Scheme 11 are correct with respect to elemental composition and valency and we believe that these structures are reasonable. Pathway I involves a retro-Diels-Alder (RDA) fragmentation wherein bonds 1 and 3 undergo scission leading to the formation of the $^{0,3}A^+$ and $^{0,3}B^+ - 2H$ ions of m/z 153 and 133, respectively, as shown in Scheme 3 of Claeys and co-workers [41]. In pathway II, the $^{0,2}B^+$ ion species of m/z 121 originates from kaempferol protonated at the C-2

position while the $^{0,2}A^+$ ion species of m/z 165 originates from kaempferol protonated at the C-3 position [41].

In Scheme 2, the ion of m/z 127 was identified previously [41] as the $^{1,4}A^+ - 2H$ ion, $C_6H_7O_3^+$. However, accurate mass measurement of this species in the product ion mass spectrum of protonated kaempferol (Table 1) gave a mass/charge ratio of 127.0522 that differs by 12.7 mDa (100 ppm) from the calculated mass/charge ratio. The magnitude of this mass difference is some 4× the largest mass difference listed in Table 1. We identify m/z 127 as $C_{10}H_7^+$ in Table 1 (and in Scheme 9) where the observed mass/charge ratio differs by but –2.6 mDa from the calculated mass/charge ratio. The peak shape for m/z 127 is

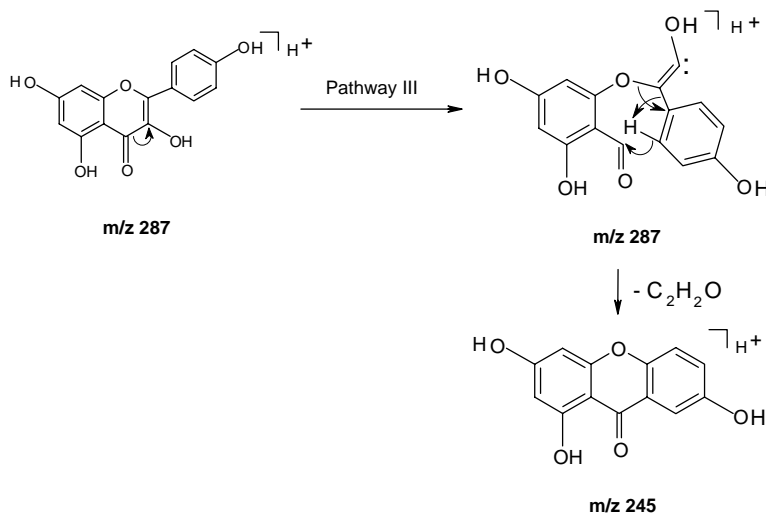
Scheme 3. Mechanism proposed for the formation m/z 245 ions from protonated kaempferol.

Table 1

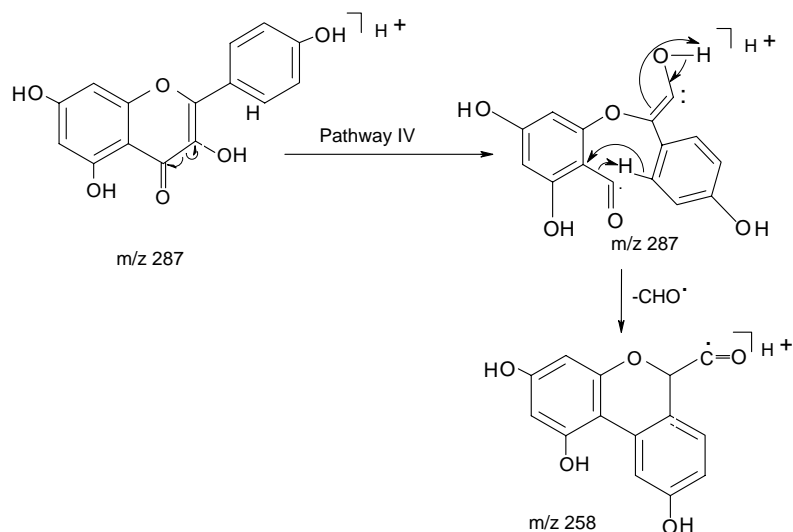
Formula, observed and calculated mass, double bond equivalents (DBE), and mass error of the fragment ions in the product ion mass spectrum of protonated kaempferol

Predicted formula	Observed mass (Da)	Calculated mass (Da)	DBE	Error (mDa)	Error (ppm)
C ₁₅ H ₁₁ O ₆ ⁺	287.0556	287.0556	10.5	0.0	0.0
C ₁₅ H ₉ O ₅ ⁺	269.0481	269.0450	11.5	+3.1	11.5
C ₁₄ H ₁₁ O ₅ ⁺	259.0635	259.0606	9.5	+2.9	11.0
C ₁₄ H ₁₀ O ₅ ⁺	258.0555	258.0528	10.0	+2.7	10.4
C ₁₄ H ₉ O ₅ ⁺	257.0430	257.0450	10.5	-2.0	-7.8
C ₁₃ H ₉ O ₅ ⁺	245.0530	245.0450	9.5	+8.0	33.0
C ₁₄ H ₉ O ₄ ⁺	241.0519	241.0501	10.5	+1.8	7.5
C ₁₃ H ₁₁ O ₄ ⁺	231.0616	231.0657	8.5	-4.1	-18.0
C ₁₃ H ₁₀ O ₄ ⁺	230.0540	230.0579	9.0	-3.9	-17.0
C ₁₃ H ₉ O ₄ ⁺	229.0451	229.0501	9.5	-5.0	-22.0
C ₁₂ H ₉ O ₄ ⁺	217.0491	217.0501	8.5	-1.0	-4.5
C ₁₃ H ₉ O ₃ ⁺	213.0557	213.0552	9.5	+0.5	2.2
C ₁₂ H ₁₁ O ₃ ⁺	203.0690	203.0708	7.5	-1.8	-9.0
C ₁₁ H ₇ O ₄ ⁺	203.0364	203.0344	8.5	+2.0	9.7
C ₁₂ H ₉ O ₂ ⁺	185.0620	185.0603	8.5	+1.7	9.4
C ₁₁ H ₇ O ₂ ⁺	171.0440	171.0446	8.5	-0.6	-3.5
C ₈ H ₅ O ₄ ⁺	165.0184	165.0188	6.5	-0.4	-2.3
C ₁₁ H ₉ O ⁺	157.0667	157.0653	7.5	+1.4	8.7
C ₇ H ₅ O ₄ ⁺	153.0188	153.0188	5.5	0.0	0.0
C ₉ H ₇ O ₂ ⁺	147.0463	147.0446	6.5	+1.7	12.0
C ₇ H ₅ O ₃ ⁺	137.0246	137.0239	5.5	+0.7	5.3
C ₇ H ₃ O ₃ ⁺	135.0072	135.0082	6.5	-1.0	-7.5
C ₈ H ₅ O ₂ ⁺	133.0294	133.0290	6.5	+0.4	3.3
C ₁₀ H ₉ ⁺	129.0703	129.0704	6.5	-0.1	-1.0
C ₁₀ H ₈ ⁺	128.0614	128.0626	7.0	-1.2	-9.4
C ₆ H ₇ O ₃ ⁺	127.0522 ^a	127.0395	3.5	[12.7]	[100]
C ₁₀ H ₇ ⁺	127.0522 ^b	127.0548	7.5	-2.6	-20
C ₁₀ H ₇ ⁺	127.0536 ^c	127.0548	7.5	-1.2	-9.3
C ₆ H ₅ O ₃ ⁺	125.0263	125.0239	4.5	+2.4	19.0
C ₇ H ₅ O ₂ ⁺	121.0298	121.0290	5.5	+0.8	7.0
C ₆ H ₅ O ₂ ⁺	109.0280	109.0290	4.5	-1.0	-8.8
Average				1.9	9.9

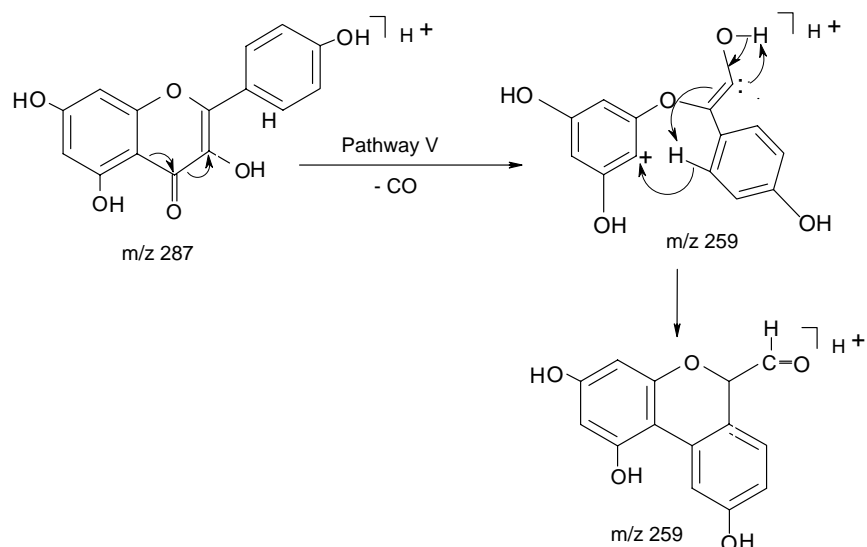
^a The mass errors associated with the identification of C₆H₇O₃⁺ have not been included in the calculation of the average errors.

^b *m/z* 127 in Scheme 2 is identified as C₁₀H₇⁺.

^c *m/z* 127 in Scheme 11 is identified also as C₁₀H₇⁺.



Scheme 4. Mechanism proposed for the formation of *m/z* 258 ions from protonated kaempferol.



Scheme 5. Mechanism proposed for the formation of m/z 259 ions from protonated kaempferol.

symmetric and does not show a shoulder on the low mass side that would indicate the possible presence of $\text{C}_6\text{H}_7\text{O}_3^+$.

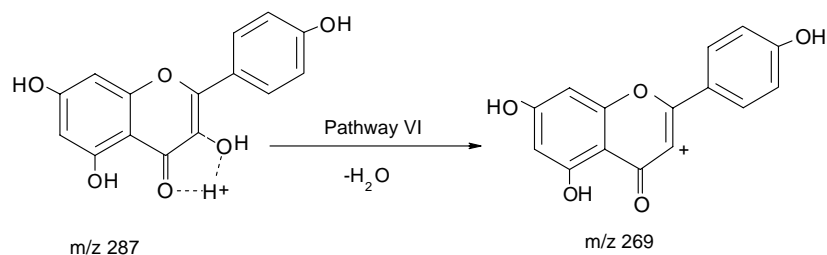
Pathway III, shown in Scheme 3, involves initially scission of the three bond in the C-ring and bond formation between the 6'-carbon of the B ring and the 4-carbon of the C ring; carbons 2 and 3 of the C-ring along with the OH group attached to C-3 are ejected as ketene. Finally, bond formation between 1'-C and the oxygen atom of ring C occurs to form the fused ring system of m/z 245.

Pathways IV and V are similar in that the CO moiety in the C-ring is lost in each case and the A- and B-rings become bonded together to form a fused system of three rings. In pathway IV, shown in Scheme 4, the initial ejection of a CHO^\bullet radical is followed by rotation of the B-ring and bonding of the 2'-C of the C-ring with the A-ring to form the fused ring structure of m/z 258. The carbon atom of the aldehyde group attached to the C-ring is C-3 from the original C-ring. In pathway V, shown in Scheme 5, the ejection of CO is followed by B-ring rotation and bonding with the A-ring to form the fused ring structure of m/z 259. Dehydration of protonated kaempferol to form a carbocation of m/z 269 is depicted as pathway VI shown in Scheme 6. It is proposed that a proton attached to the keto oxygen atom at C-4 of the C-ring combines with the vicinal hydroxy

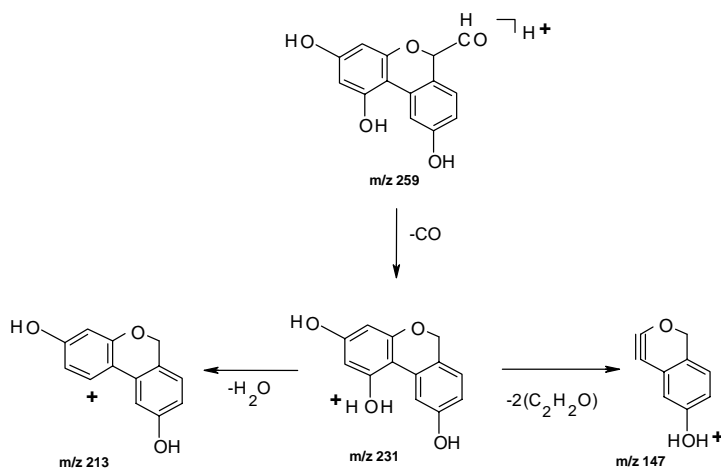
group and the resulting molecule of water is ejected. The carbocation structure for m/z 269 differs from the charged ether structure proposed elsewhere [41].

The secondary fragmentations, or fragmentations of the primary product ions, are discussed in order of descending mass/charge ratio of the primary product ions shown in Scheme 2. Fragment ions generated at enhanced cone voltages upstream of the first mass-resolving element were subjected to CID so as to identify the direct product ion-precursor ion relationship. The utilization of enhanced cone voltage to maximize first generation fragment ion signal intensity can yield pseudo-MS/MS performance in the Q-TOF IITM mass spectrometer that is useful in determining the hierarchy of fragment ions. In the examination of a standard substance such as kaempferol, the probability of isolating more than one isobaric fragment ion species in the first quadrupole mass filter is zero when such ions are not detected in the initial product ion mass spectrum. The ion species m/z 133, 127, and 121 were not examined further.

The dissociation of m/z 259, as shown in Scheme 7, occurs by loss of CO to yield m/z 231. The extrusion of CO is a characteristic process of protonated and deprotonated flavonoids. The ion of m/z 231, in turn, fragments by both the loss of H_2O to yield the carbocation of m/z 213 and,



Scheme 6. Mechanism proposed for the formation of m/z 269 ions from protonated kaempferol.

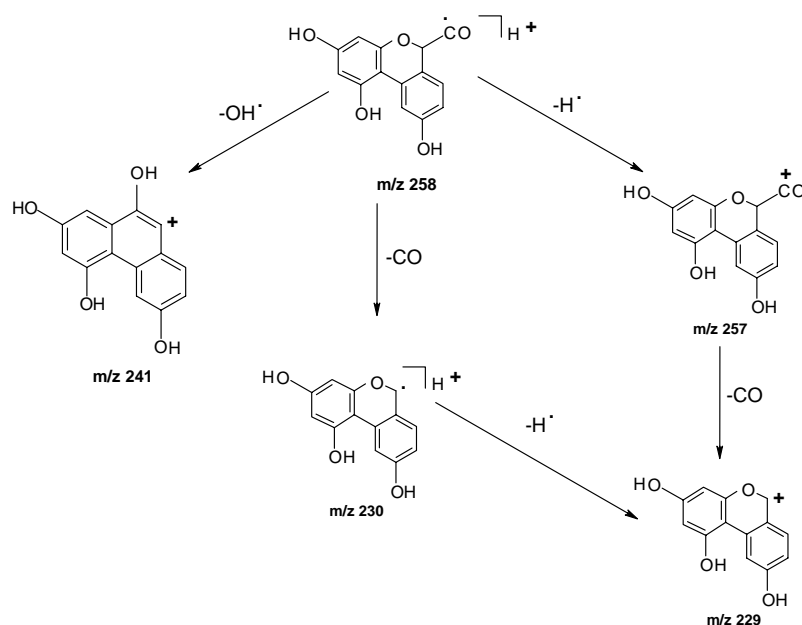
Scheme 7. Fragmentation of m/z 259 and of m/z 231 from protonated kaempferol.

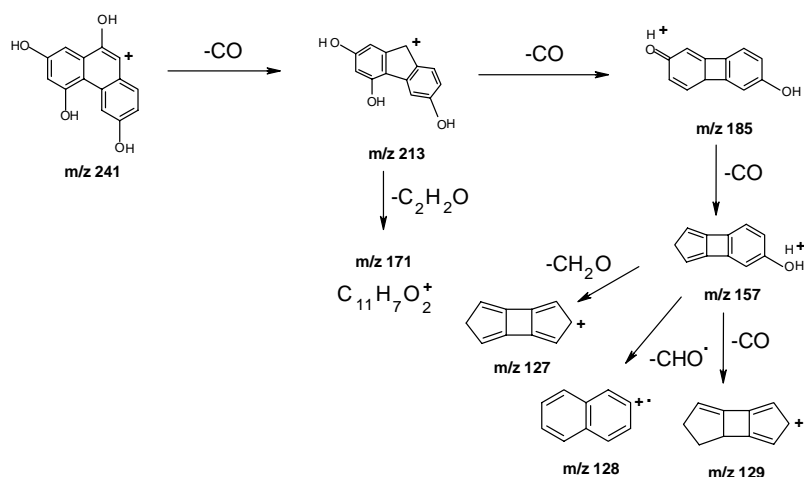
presumably, the loss of two ketene molecules to yield the protonated phenol of m/z 147. In Scheme 8 is shown the fragmentation of m/z 258 by loss of H^\bullet , OH^\bullet , and CO . Although the loss of a hydrogen atom (to form m/z 257) is somewhat unusual, the loss of a hydroxyl radical (to form m/z 241) is observed frequently in the fragmentation of hydroxyflavonoids. The ion of m/z 229 was observed both as a result of hydrogen atom loss from m/z 230 and by the loss of a CO molecule from m/z 257. Because the observed mass/charge ratio for m/z 229 was the same (m/z 229.0451 and 229.0450) in each case, it was assumed that the same carbocation structure was obtained in each case.

The relatively high ion signal intensity of m/z 241 from m/z 258 permitted further examination of this ion species. The fragmentation of m/z 241 is shown in Scheme 9. It was

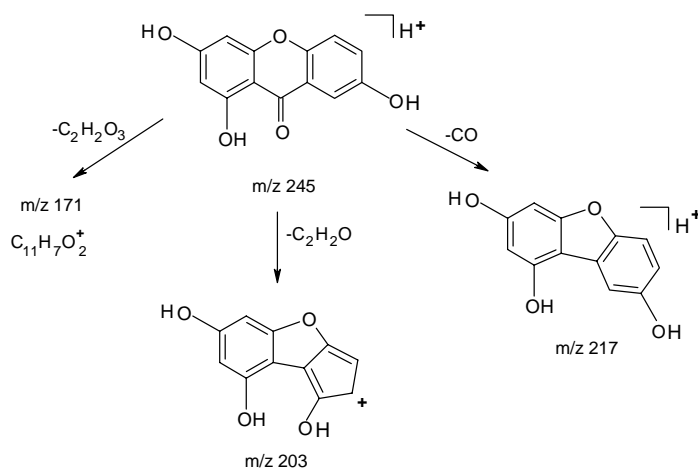
observed (by isolation and CID of the precursor ion) that CO is lost from each of the ion species m/z 241, 213, 185, and 157 in turn. The loss of the final CO molecule from m/z 157 is competitive with losses of CHO^\bullet and CH_2O to form m/z 129, 128, and 127, respectively. On the basis of accurate mass measurements and corresponding elemental compositions (Table 1), the elemental composition of m/z 127 shown in Scheme 9 is $\text{C}_{10}\text{H}_7^+$. The observation of m/z 171 from m/z 213 is assumed to be due to the loss of ketene.

CID of m/z 245 yielded three fragment ion species as shown in Scheme 10. The product ion of m/z 171 observed here has the same elemental composition as that from m/z 213 in Scheme 9. The remaining ion species were m/z 203 and m/z 217 formed by loss of ketene and CO , respectively. The structure proposed for m/z 203 and shown in Scheme 10

Scheme 8. Fragmentation of m/z 258, m/z 257, m/z 230 from protonated kaempferol.



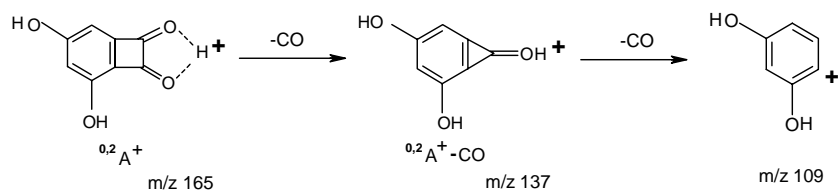
Scheme 9. Fragmentation of m/z 241 and of three other ion species obtained from m/z 241. The elemental composition is given for m/z 171 for which a structure has not been proposed.



Scheme 10. Fragmentation of m/z 245 from protonated kaempferol.

is based on an elemental composition of $C_{11}H_7O_4^+$ obtained by accurate mass measurement. However, an accurate mass measurement of the ion signals obtained for m/z 203 in the product ion mass spectrum of protonated kaempferol (Fig. 1) was consistent with an elemental composition of $C_{12}H_{11}O_3^+$. Supporting evidence for the former isobar was obtained from the observed loss of CO from m/z 231 of elemental composition $C_{13}H_{11}O_4^+$.

Further evidence for the loss of oxygen atoms as CO molecules is shown in Scheme 11 that shows the successive fragmentation of m/z 165 ($^{0,2}A^+$) and m/z 137. The structure given in Scheme 11 for m/z 137 is that proposed earlier [41].

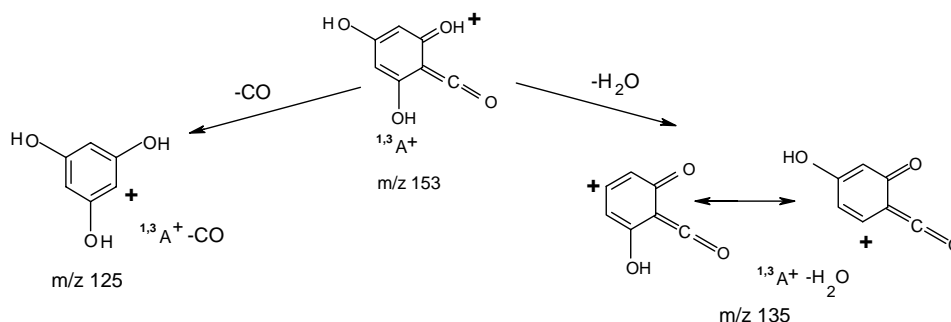


Scheme 11. Fragmentation of m/z 165 and of m/z 137 from protonated kaempferol.

The $^{1,3}A^+$ ion of m/z 153 from protonated kaempferol shows competing losses of CO and H_2O , as shown in Scheme 12 to yield the carbocations of m/z 125 and 135, respectively. The structure given in Scheme 12 for m/z 153 is that proposed earlier [41]. The fragment ion structures proposed in the above schemes are plausible on the basis of chemical intuition but are not definitive.

3.3. Deprotonated kaempferol, $[M - H]^-$

In the report of an earlier examination of deprotonated kaempferol [35], we had stated that the dissociation of

Scheme 12. Fragmentation of m/z 153 from protonated kaempferol.

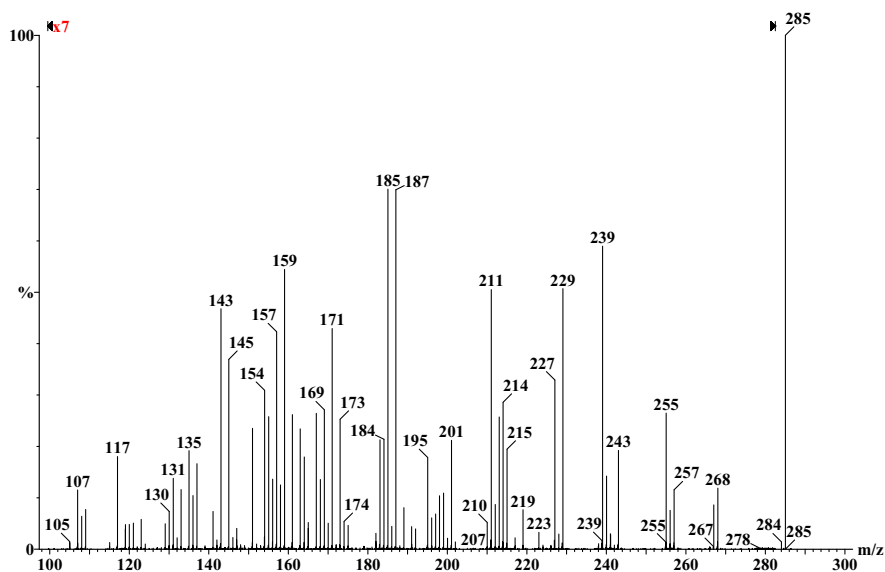
$[M - H]^-$ ions occurred precipitously at a collision energy of 25 eV with the formation of some 60 fragment ions of low ion signal intensity. Further examination has shown that, by careful variation of the collision energy and by prolonged collection of ion signals, the principal fragmentation processes can be identified. The product ion mass spectrum of $[M - H]^-$ ions of kaempferol obtained at a collision energy of 26 eV is shown in Fig. 2. More than 70 fragment ion species are evident in this figure.

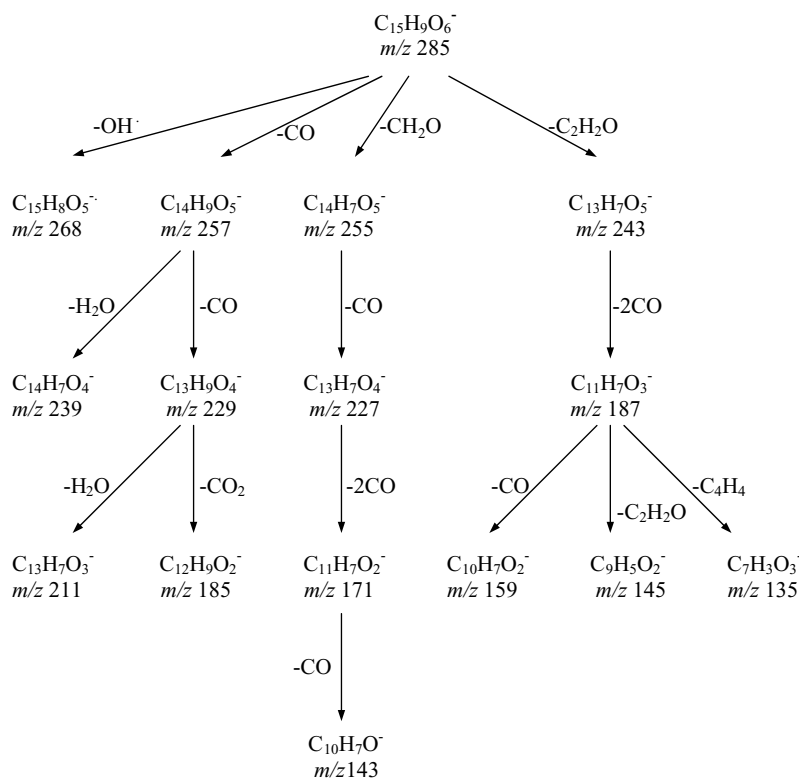
The fragment ion of m/z 151 was observed at a collision energy of 15 eV; this energy is the lowest at which any fragment ion signal was observed. It is proposed that this species is the $^{1,3}A^-$ ion. The negative ion counterpart of the $^{1,3}A^+$ ion of m/z 153 ($C_7H_5O_4^+$, Scheme 2) is expected to have a mass/charge ratio of 151; accurate mass measurement m/z 151 showed that the elemental composition was $C_7H_3O_4^-$ as would be expected. The elemental compositions for a further 15 negative ion species were obtained by accurate mass measurement and are shown in Table 2. In Table 2 are tabulated the formula, observed mass, calculated mass, double bond equivalents, and mass error for the fragment ions observed in the product ion mass spec-

Table 2

Formula, observed and calculated mass, double bond equivalents (DBE), and mass error of the fragment ions in the product ion mass spectrum of deprotonated kaempferol, $[M - H]^-$

Predicted formula	Observed mass (Da)	Calculated mass (Da)	DBE	Error (mDa)	Error (ppm)
$C_{15}H_9O_6^-$	285.0399	285.0399	11.5	0.0	0.0
$C_{15}H_8O_5^-$	268.0388	268.0372	12.0	+1.6	+6.1
$C_{14}H_9O_5^-$	257.0471	257.0450	10.5	+2.1	+8.2
$C_{14}H_7O_5^-$	255.0302	255.0293	11.5	+0.9	+3.3
$C_{13}H_7O_5^-$	243.0324	243.0293	10.5	+3.1	+13.0
$C_{14}H_7O_4^-$	239.0374	239.0344	11.5	+3.0	+12.0
$C_{13}H_9O_4^-$	229.0533	229.0501	9.5	+3.2	+14.0
$C_{13}H_7O_4^-$	227.0377	227.0344	10.5	+3.3	+14.0
$C_{13}H_7O_3^-$	211.0419	211.0395	10.5	+2.4	+11.0
$C_{11}H_7O_3^-$	187.0399	187.0395	8.5	+0.4	+2.0
$C_{12}H_9O_2^-$	185.0604	185.0603	8.5	+0.1	+0.8
$C_{11}H_7O_2^-$	171.0432	171.0446	8.5	-1.4	-8.2
$C_{10}H_7O_2^-$	159.0439	159.0446	7.5	-0.7	-4.4
$C_7H_3O_4^-$	151.0020	151.0031	6.5	-1.1	-7.5
$C_9H_5O_2^-$	145.0303	145.0290	7.5	+1.3	9.3
$C_{10}H_7O^-$	143.0466	143.0497	7.5	-3.1	-22.0
$C_7H_3O_3^-$	135.0081	135.0082	6.5	-0.1	0.9
Average				1.7	8.5

Fig. 2. Product ion mass spectrum of deprotonated kaempferol, $[M - H]^-$, obtained at a laboratory frame collision energy of 26 eV.

Scheme 13. Proposed fragmentation scheme for kaempferol $[M - H]^-$.

trum of deprotonated kaempferol. The errors between the observed masses and calculated ones ranged from 0.1 to 3.3 mDa (0.9–14.0 ppm) with an average value of 1.7 mDa (8.5 ppm) indicating, again, good mass accuracy.

The low ion signal intensity for negative ion fragments mitigated against facile observation of their product ion mass spectra. However, by examination of the elemental compositions of these ions and upon consideration of probable neutral moiety losses of OH^\bullet , CO, H_2O , CH_2O , and ketene, it is possible to relate many of the fragment ions to their immediate precursors. The proposed fragmentation pattern for $[M - H]^-$ is shown in Scheme 13.

4. Conclusion

Low-energy product ion mass spectra of the $[M+H]^+$ and $[M - H]^-$ ions of kaempferol showed simple fragmentation patterns that permitted characterization of the substituents in the A and B rings. Fragmentation mechanisms and ion structures have been proposed. The use of elevated cone voltages permitted observation of product ion mass spectra of selected primary fragment ions. The examination of product ion mass spectra at high mass resolution allowed unambiguous determination of the elemental composition of fragment ions and resolution of two pairs of isobars. Characterization of the fragmentation patterns for $[M+H]^+$ and $[M - H]^-$ ions of kaempferol is facilitating a current investigation of flavonoid glycosides in this laboratory.

Acknowledgements

The authors acknowledge the financial support from each of the Natural Sciences and Engineering Research Council of Canada (Discovery Grants Program), the Canada Foundation for Innovation, the Ontario Research & Development Challenge Fund and Trent University.

References

- [1] J.B. Harborne (Ed.), *The Flavonoids: Advances in Research Since 1986*, Chapman and Hall, London, 1994.
- [2] E. Sjöström, *Wood Chemistry Fundamentals and Applications*, Academic Press, New York and London, 1981.
- [3] E.C. Bate-Smith, in: W.E. Hillis (Ed.), *Wood Extractives and Their Significance to the Pulp and Paper Industries*, Academic Press, New York and London, 1962, p. 133.
- [4] R.S. Kaldras, C.L. Hughes, *Reprod. Toxicol.* 3 (1989) 81.
- [5] K.D.R. Setchell, in: J.A. McLachlan (Ed.), *Estrogens in the Environment II. Influences on Development*, Elsevier, Amsterdam, 1985, p. 66.
- [6] J.B. Harborne, R.J. Grayer, in: J.B. Harborne (Ed.), *The Flavonoids: Advances in Research Since 1986*, Chapman and Hall, London, 1994, p. 589.
- [7] R. Miksicek, *J. Mol. Pharm.* 44 (1993) 37.
- [8] J.D.J. Kellis, L.E. Vickery, *Science* 225 (1984) 1032.
- [9] L. Packer, G. Rimach, F. Virgili, *Free Radic. Biol. Med.* 27 (1999) 704.
- [10] R.A. Dixon, C.L. Steele, *Trends Plant Sci.* 4 (1999) 394.
- [11] Y.C. Park, G. Rimach, C. Saliou, G. Valacchi, L. Packer, *FEBS Lett.* 465 (2000) 93.

- [12] S.E. Nielsen, R. Freese, C. Cornett, L.O. Dragsted, *Anal. Chem.* 72 (2000) 1503.
- [13] D. Romanová, D. Grandai, B. Jókóvá, P. Bodek, A. Vachálková, *J. Chromatogr. A* 870 (2000) 463.
- [14] M. Careri, L. Elviri, A. Mangia, *Rapid Commun. Mass Spectrom.* 13 (1999) 2399.
- [15] C.J. van Platerink, T.P.J. Mulder, P.J.W. Schuyf, J.M.M. van Amelsvoort, in: *Proceedings of the 48th ASMS Conference on Mass Spectrometry and Allied Topics*, Long Beach, CA, 2000.
- [16] X.-G. He, L.-Z. Lian, L.-Z. Lin, M.W. Bernart, *J. Chromatogr. A* 791 (1997) 127.
- [17] N. Chaves, J.J. Ríos, C. Gutierrez, J.C. Escudero, J.M. Olías, *J. Chromatogr. A* 799 (1998) 111.
- [18] X. He, L. Lin, L. Lian, *J. Chromatogr. A* 755 (1996) 127.
- [19] P. Bednarek, L. Kerhoas, P. Wojtaszek, J. Einhorn, M. Stobiecki, in: *Proceedings of the 15th International Mass Spectrometry Conference*, Barcelona, Spain, 27 August–1 September 2000.
- [20] Y.-L. Ma, I. Vedernikova, H. Van den Heuvel, M. Claeys, *J. Am. Soc. Mass Spectrom.* 11 (2000) 136.
- [21] B.J. Boersma, R.P. Patel, M. Kirk, P.L. Jackson, D. Muccio, V.M. Darley-Usmar, S. Barnes, *Arch. Biochem. Biophys.* 368 (1999) 265.
- [22] R. Franski, W. Bylka, I. Matlawska, M. Stobiecki, in: *Proceedings of the 15th International Mass Spectrometry Conference*, Barcelona, Spain, 27 August–1 September 2000.
- [23] F. Cuyckens, Y.-L. Ma, H. Van den Heuvel, M. Claeys, in: *Proceedings of the 15th International Mass Spectrometry Conference*, Barcelona, Spain, 27 August–1 September 2000.
- [24] M.A. Almoester-Ferreira, P. Esperança, M.C. Oliviera, in: *Proceedings of the 15th International Mass Spectrometry Conference*, Barcelona, Spain, 27 August–1 September 2000.
- [25] C. Cren-Olivé, S. Deprez, B. Coddeville, C. Rolando, in: *Proceedings of the 15th International Mass Spectrometry Conference*, Barcelona, Spain, 27 August–1 September 2000.
- [26] M.T. Fernandez, M.L. Mira, M.H. Florêncio, K.R. Jennings, in: *Proceedings of the 15th International Mass Spectrometry Conference*, Barcelona, Spain, 27 August–1 September 2000.
- [27] Y.Y. Lin, K.J. Ng, J. Kwokei, S. Yang, *J. Chromatogr.* 629 (1993) 389.
- [28] M.S. Lee, D.J. Hook, E.H. Kerns, K.J. Volk, I.E. Rosenberg, *Biol. Mass Spectrom.* 22 (1993) 84.
- [29] M. Saegesser, M. Meinzer, *J. Am. Soc. Brew. Chem.* 54 (1996) 129.
- [30] A. Raffaelli, G. Moneti, V. Mercati, E. Toja, *J. Chromatogr. A* 777 (1997) 223.
- [31] S. Chimichi, V. Mercati, G. Moneti, A. Raffaelli, E. Toja, *Nat. Prod. Lett.* 11 (1998) 225.
- [32] J.F. Stevens, A.W. Taylor, M.L. Deinzer, *J. Chromatogr. A* 832 (1/2) (1999) 97.
- [33] B. Ameer, R.A. Weintraub, J.V. Johnson, R.A. Yost, R.L. Rouseff, *Clin. Pharmacol. Ther. (St. Louis)* 60 (1996) 34.
- [34] J.F. Stevens, E. Wollenweber, M. Ivancic, V.L. Hsu, S. Sundberg, M.L. Deinzer, *Phytochemistry* 51 (1999) 771.
- [35] R.J. Hughes, T.R. Croley, C.D. Metcalfe, R.E. March, *Int. J. Mass Spectrom.* 210/211 (2001) 371.
- [36] T.R. Croley, R.J. Hughes, C.D. Metcalfe, R.E. March, *Rapid Commun. Mass Spectrom.* 14 (2000) 1494.
- [37] T.R. Croley, R.J. Hughes, C. Hao, C.D. Metcalfe, R.E. March, *Rapid Commun. Mass Spectrom.* 14 (2000) 2154.
- [38] T.J. Mabry, K.R. Markham, in: J.B. Harborne, T.J. Mabry, H. Mabry (Eds.), *The Flavonoids*, Academic Press, New York, 1975, p. 78.
- [39] A. Baracco, G. Bertin, E. Gnocco, M. Legorati, S. Sedocco, S. Catinella, D. Favretto, P. Traldi, *Rapid Commun. Mass Spectrom.* 9 (1995) 427.
- [40] C.G. de Koster, W. Heerma, G. Dijkstra, G.J. Niemann, *Biomed. Mass Spectrom.* 12 (1985) 596.
- [41] Y.L. Ma, Q.M. Li, H. Van den Heuvel, M. Claeys, *Rapid Commun. Mass Spectrom.* 11 (1997) 1357.
- [42] B. Domon, C. Costello, *Glycoconjug. J.* 5 (1988) 397.